IJC Heart & Vasculature 48 (2023) 101269

Contents lists available at ScienceDirect

IJC Heart & Vasculature

journal homepage: www.sciencedirect.com/journal/ijc-heart-and-vasculature

CD47 blockade enhances phagocytosis of cardiac cell debris by neutrophils

Elias Haj-Yehia [a,1], Sebastian Korste [a,1], Robert Jochem [b], Aldona Lusha [a], Anna Roth [a], Nina Dietzel [a], Josefine Niroomand [a], Pia Stock [a], Astrid M. Westendorf [c], Jan Buer [c], Ulrike B. Hendgen-Cotta [a], Tienush Rassaf [a], Matthias Totzeck [a,*]

[a] Department of Cardiology and Vascular Medicine, West German Heart and Vascular Center, University Hospital Essen, 45147 Essen, Germany
[b] Department of Nephrology, University Hospital Essen, 45147 Essen, Germany
[c] Institute of Medical Microbiology, University Hospital Essen, University of Duisburg-Essen, Essen, Germany

ARTICLE INFO

Keywords:
CD47
Ischemia/reperfusion injury
Reperfused acute myocardial infarction
repAMI
Neutrophils
Phagocytosis

ABSTRACT

CD47 is a cell surface protein controlling phagocytotic activity of innate immune cells. CD47 blockade was investigated as an immune checkpoint therapy in cancer treatment, enhancing phagocytosis of tumor cells by macrophages. Anti-CD47 treatment also reduced injury size during reperfused acute myocardial infarction (repAMI) by enhancing phagocytotic acitivity of macrophages. Little is known about the impact of CD47 blockade on neutrophils, representing the main portion of early infiltrating immune cells after repAMI. Therefore, we performed 45 min of cardiac ischemia followed by 24 h of reperfusion, observing a decreased cardiac injury size measured by triphenyl tetrazolium chloride (TTC) Evan's blue staining. We were able to detect this effect with an innovative three-dimensional method based on light sheet fluorescence microscopy (LSFM). This further allowed us a simultaneous analysis of neutrophil infiltration, showing an unaltered amount of injury-associated neutrophils with reduced cardiac injury volume from repAMI. This observation suggests modulated phagocytosis of cell debris by neutrophils. Therefore, we performed flow cytometry analysis, revealing an increased phagocytotic activity of neutrophils *in vitro*. These findings highlight that CD47 blockade also enhances phagocytosis of cardiac cell debris by neutrophils, which might be an additional protective effect of anti-CD47 treatment after repAMI.

1. Introduction

Reperfused acute myocardial infarction (repAMI) provokes a mobilization and infiltration of various immune cells into the heart at different time points [1]. One of the first cell types infiltrating the affected myocardium are neutrophils [2]. In the context of repAMI, they display different, partially ambivalent effects. On one hand, they orchestrate subsequent remodeling processes driven by other immune cells [3,4]. On the other hand, they produce reactive oxygen species (ROS) and extracellular traps (NETs), which are known to be cytotoxic and pro-inflammatory augmenting cardiac reperfusion injury [5,6]. Inhibition of both aspects seems to be cardioprotective [5,7].

Besides, one important function of neutrophils during repAMI is phagocytosis of cardiac cell debris [3]. Sufficient clearance of necrotic and apoptotic debris by immune cells is an important aspect limiting infarct size after repAMI [8]. Since insufficient debris removal provokes expansion of infarct size and worsens cardiac remodeling, optimal phagocytotic activity of infiltrating immune cells during repAMI is essential to limit development of heart failure [9,10].

One pivotal factor controlling phagocytosis is CD47 [11,12]. This ubiquitous expressed cell surface protein inhibits phagocytotic activity through interaction with its immune cell receptor signal regulatory protein α (SIRP-α) [13,14]. Targeting interaction between CD47 and SIRP-α is mainly investigated as an immune checkpoint in cancer treatment [11,15–17]. Inhibition of this interaction leads to an increasing phagocytosis of tumor cells by macrophages [12,16,18]. SIRP- α deficiency also enhances phagocytotic activity of neutrophils during lung cancer [19]. In the context of repAMI it was also shown that inhibition of CD47 enhances phagocytosis of cardiac cell debris by macrophages leading to a reduced infarction area [20]. CD47 blockade decreased injury size in other ischemia/reperfusion models, whereas other factors like reduction of ROS production and inflammatory

* Corresponding author.
E-mail address: matthias.totzeck@uk-essen.de (M. Totzeck).
[1] These authors contributed equally to this work.

https://doi.org/10.1016/j.ijcha.2023.101269
Received 4 August 2023; Received in revised form 1 September 2023; Accepted 5 September 2023
Available online 9 September 2023

cytokine secretion mediated these effects [21,22].

The impact of CD47 on neutrophil phagocytotic activity and acute clearance of cell debris during repAMI is not examined so far. We hypothesize that in this context, CD47 blockade enhances phagocytosis of cardiac cell debris by neutrophils, which might support acute clearance of cardiac cell debris leading to reduced infarct size.

2. Methods

2.1. Animals and ethical statement

Male C57BL/6JRJ wild-type mice (12 ± 3 weeks of age) were housed in the central animal facility of the University Hospital Essen at a 12 h/12 h day-night-cycle. They had access to food and water ad libitum before and during the experiments. For Langendorff experiments male $CD47^{-/-}$ knockout mice (12 ± 3 weeks of age) were additionally purchased from Jackson laboratories (Strain number #003173, Bar Arbor, ME, USA) and held under the same conditions. All experiments were approved beforehand by the ethical committee of the Landesamt für Natur-, Umwelt- und Verbraucherschutz (LANUV).

2.2. Ischemia/Reperfusion (I/R) heart injury

Male C57BL/6JRJ (12 ± 3 weeks of age) were subjected to a published *in vivo* myocardial I/R protocol [23,24]. Briefly, mice were anesthetized by intraperitoneal injection of ketamine (100 mg/kg, belapharm, Vechta, Germany) and xylazin (10 mg/kg, Ceva Tiergesundheit, Düsseldorf, Germany). After oral intubation they were ventilated throughout the operation procedure, with 0.8 l/min air and 0.2 l/min O_2 at a tidal volume of 250 μL/stroke and a breathing frequency of 140 S/min. During the operation anesthesia was maintained by supplementing 2 % isoflurane (Piramal, Mumbai, India). For induction of I/R injury the chest was opened through a left lateral thoracotomy and the left coronary artery (LCA) was ligated. After 45 min of ischemia, reperfusion was allowed for 24 h. In the postoperative phase mice were treated with 0.1 mg/kg buprenorphine (Indivior, Chesterfield Court House, VA, USA) subcutaneously every 8 h until sacrifice following cervical dislocation.

2.3. In vivo CD47 antibody treatment

5 min before reperfusion mice received a single dose of monoclonal anti-CD47 antibody (30 mg/kg KG, clone: mIAP301) or IgG2a (30 mg/kg KG, clone: 2A3; both BioXCell, Lebanon, NH, USA) via injection into the left ventricular cavity as previously described [25]. Injection volume did not exceed 100 μL.

2.4. 2,3,5-Triphenyltetrazolium chloride (TTC) Evan's blue staining

TTC and Evan's blue staining were used to quantify the size of reperfused acute myocardial infarction (repAMI) as described previously [23,26]. After removal, hearts were flushed blood-free with PBS (Sigma-Aldrich, St. Louis, MO, USA) via cannulation of the ascending aorta. Then LCA was re-occluded by suture followed by injection of 1 mL 1 % Evan's blue dye (Sigma-Aldrich, St. Louis, MO, USA) to visualize the area at risk (AAR). Thereafter, the heart was seperated into 1–2 mm transversal cross-sections and incubated in 1 % TTC in 0.0774 M Na_2HPO_4 (Carl Roth, Karlsruhe, Germany) and 0.0226 M NaH_2PO_4 (-Sigma-Aldrich, St. Louis, MO, USA) at 37 °C for 5 min. Images were obtained with a M80 microscope and IC80 HD camera (Leica, Wetzlar, Germany) following analysis by a blinded investigator using ImageJ 1.53 (NIH, New York City, NY, USA) [27].

2.5. Ex vivo Langendorff model

Mice were anesthetized using isoflurane and euthanized in narcosis by cervical dislocation, hearts were rapidly excised and immediately immersed in ice-cold Krebs-Henseleit buffer, comprised of 118 mM NaCl (Carl Roth, Karlsruhe, Germany), 25 mM $NaHCO_3$ (Carl Roth, Karlsruhe, Germany), 4.7 mM KCl (Carl Roth, Karlsruhe, Germany), 1.2 mM $MgSO_4$ (Carl Roth, Karlsruhe, Germany), 1.2 mM KH_2PO_4 (Carl Roth, Karlsruhe, Germany), 11 mM D-glucose (Sigma-Aldrich, St. Louis, MO, USA) and 1.4 mM $CaCl_2$ (Carl Roth, Karlsruhe, Germany). The ascending aorta was cannulated, and the heart was mounted on a Langendorff apparatus and perfused retrogradely through the aorta with Krebs-Henseleit buffer, which was constantly gas-flushed with 95 % O_2 and 5 % CO_2 (pH 7.4 at 37 °C). Perfusion was maintained at a constant pressure of 80 mmHg. Coronary flow rate (ml/min) was measured constantly and hearts with a flow rate below 2 mL/min during stabilization period were excluded from the study. Prior to global ischemia, the isolated hearts were allowed to equilibrate at 37 °C for 20 min. Following stabilization, the flow of the perfusion buffer was diverted from the heart to the reservoir for 30 min. Reperfusion was instigated by reverting the flow back to the heart and was confirmed by an increase (within the first minute) of the coronary flow rate. Reperfusion continued for 120 min. After that, hearts were cut into 1–2 mm transversal cross-sections and incubated in 1 % TTC in 0.0774 M Na_2HPO_4 (Carl Roth, Karlsruhe, Germany) and 0.0226 M NaH_2PO_4 (Sigma-Aldrich, St. Louis, MO, USA) at 37 °C for 5 min. Images were obtained with a M80 microscope and IC80 HD camera (Leica, Wetzlar, Germany) following analysis by a blinded investigator using ImageJ 1.53 (NIH, New York City, NY, USA) [27].

2.6. In vitro human cardiac myocyte hypoxia/reoxygenation model

Human Cardiac Myocytes (hCM) were obtained from Promocell (Promocell, Heidelberg, Germany) and cultured in Myocyte Growth Medium (Promocell, Heidelberg, Germany) mixed with supplied supplement, 50 ng/ml amphotericin B (Promocell, Heidelberg, Germany) and 50 μg/ml gentamycin (Invitrogen, Waltham, MA, USA). In brief, cells were seeded at 1×10^5 cells/cm^2 and split using the Promocell DetachKit (Promocell, Heidelberg, Germany) every time the culture reached 90–100 % confluency. For the experiment in this study, cells from passage 5–7 were used.

For the hypoxia/reoxygenation model, cells were seeded into 6-well plates at 1×10^5 cells/cm^2 and incubated as described before until the culture reached close to 100 % confluency. For each set of experiments two 6-well plates were used, one for hypoxia and one as normoxia control. For hypoxia, cells were incubated in hypoxia buffer comprised of 113 mM NaCl (Carl Roth, Karlsruhe, Germany), 4.7 mM KCl (Carl Roth, Karlsruhe, Germany), 12 mM HEPES (Carl Roth, Karlsruhe, Germany), 1.2 mM $MgSO_4$ (Carl Roth, Karlsruhe, Germany), 30 mM Taurine (Sigma-Aldrich, St. Louis, MO, USA) and 1.3 mM $CaCl_2$ (Carl Roth, Karlsruhe, Germany) in ddH_2O at pH 7.4. To induce hypoxia, the hypoxia buffer was degassed with pure nitrogen (AirLiquid, Paris, France) for 10 min before it was added to the cells and the plate was swiftly put into a hypoxia chamber set at 1 % O_2, 5 % CO_2 and 37 °C for 20 h. The normoxia control remained in Myocyte Growth Medium at normal O_2 levels and 5 % CO_2 at 37 °C. On each plate, three wells were chosen at random for incubation with human anti-CD47 antibody (clone: B6H12) or IgG control (clone: MOPC-21; both BioXCell, Lebanon, NH, USA), both at 1 μg/ml final concentration, which were added before the start of hypoxia. Following hypoxia, medium was changed on both plates to fresh Myocyte Growth Medium and reoxygenation continued for 4 h at normal O_2 levels and 5 % CO_2 at 37 °C. Anti-CD47 and IgG control antibodies were added again at 1 μg/ml at start of reoxygenation. Hypoxia duration and buffer/medium conditions were tested in preceding experiments (Supplementary Fig. 1).

The neutral red uptake assay was used to assess cell viability. In brief, neutral red (Sigma-Aldrich, St. Louis, MO, USA) was added at 0.004 % final concentration to fresh Myocyte Growth Medium and sterile filtered. Old medium was removed from the wells and the new medium with neutral red was added for 1 h at 5 % CO_2 and 37 °C. After that, wells were washed thrice with PBS and dried at RT for 1 h. Absorbed neutral

red was removed from the cells with ice-cold isopropyl alcohol (Carl Roth, Karlsruhe, Germany) with 1 % 1 M HCl (Sigma-Aldrich, St. Louis, MO, USA). 100 µL of the colored solutions were transferred in duplicates to a 96-well plate and the extraction solution was used in two wells as blank controls. Color absorption was measured in a BMG Fluostar plate reader (BMG Labtech, Ortenberg, Germany) at 540 nm. Obtained values were blank corrected and averaged within experimental groups. A total of three sets of experiments were conducted and averages from these sets were used in the final analysis.

2.7. Flow cytometry

To create single-cell suspensions from murine left ventricular cardiac tissue, hearts were mechanically minced and incubated in an enzyme solution comprised of 450 U/mL collagenase I (Sigma Aldrich, St. Louis, MO, USA), 125 U/mL collagenase XI (Sigma Aldrich, St. Louis, MO, USA), 60 U/mL hyaluronidase (Sigma Aldrich, St. Louis, MO, USA), 20 mM HEPES (Sigma Aldrich, St. Louis, MO, USA) and 60 U/mL DNase (Sigma Aldrich, St. Louis, MO, USA) in PBS with Calcium and Magnesium ($PBS^{Ca/Mg}$ ThermoFisher Scientific, Waltham, MA, USA) for 40 min in a ThermoMixer C (Eppendorf, Hamburg, Germany) at 37 °C and 750 r.p.m. After enzymatic digestion, the solution was filtered through a 40 µm filter and flow-through was centrifuged for 5 min at 4 °C and 400 × *g*. The supernatant was discarded and the cell pellet dissolved in 1.5 mL PBS without Calcium and Magnesium ($PBS^{-Ca/-Mg}$, ThermoFisher Scientific, Waltham, MA, USA). Finally, 200 µL of this solution per sample were used for staining, while a mixture of all solutions was used for fluorescence minus one (FMO) control. Blocking of Fc-receptors was conducted by adding 2 µL of TruStain fcX (BioLegend, San Diego, CA, USA) and incubating for 10 min on ice in the dark. Samples were then washed by adding 100 µL $PBS^{-Ca/-Mg}$, centrifuging for 5 min at 4 °C and 400 × *g*, discarding the supernatant and dissolving the cell pellet in 50 µL $PBS^{-Ca/-Mg}$ containing Zombie NIR (BioLegend, San Diego, CA, USA) at a final dilution of 1:2000 for live/dead staining. Besides, samples were stained by adding 50 µL $PBS^{-Ca/-Mg}$ containing antibodies CD45-AF700 (BioLegend, San Diego, CA, USA), CD45R-BV510 (BioLegend, San Diego, CA, USA), CD3-BV510 (BioLegend, San Diego, CA, USA), Ly6G-PerCP/Cy5.5 (BioLegend, San Diego, CA, USA), CD11b-BV605 (BioLegend, San Diego, CA, USA), F4/80-BV421 (BioLegend, San Diego, CA, USA), CD31-BV421 (BioLegend, San Diego, CA, USA), CD140a-BV605 (BioLegend, San Diego, CA, USA) and CD47-PerCP/Cy5.5 (BioLegend, San Diego, CA, USA), all at a final dilution of 1:200 except CD47-PerCP/Cy5.5 (1:50). Incubation was conducted for 30 min at RT in the dark. After antibody incubation, samples were washed as before, the supernatant was discarded and the cell pellet was dissolved in 300 µL FACS-Buffer, comprised of 1 % (v/v) fetal bovine serum (PAN Biotech, Aidenbach, Germany) and 0.5 % (w/v) bovine serum albumin (Carl Roth, Karlsruhe, Germany) in $PBS^{-Ca/-Mg}$. Data were acquired on a BD FACS Aria III (BD Biosciences, San Jose, CA, USA) and analysis was performed using FlowJo 10.8.1 software (BD Life Sciences, East Rutherford, NJ, USA).

2.8. Light sheet fluorescence microscopy (LSFM)

Mice received intravenous tail vein injections 10 min before sacrifice with 10 µg of each antibody in PBS in a total volume of 150 µL per animal. For discrimination of $CD31^{neg}$ area purified anti-mouse CD31 (clone: Mec13.3, BD Bioscience, San Jose, CA, USA) was conjugated with AlexaFluor 790 using an IgG coupling kit (ThermoFisher Scientific, Waltham, MA, USA) as previously described [26]. Neutrophils were stained using anti-mouse Ly6G antibody conjugated with AlexaFluor 647 (clone: 1A8, BioLegend, San Diego, CA, USA). After sacrifice, mice were perfused blood-free with PBS, hearts were excised and subjected to chemical fixation using 10 % formalin (Morphisto, Offenbach am Rhein, Germany) while standing at 4 °C over night. Following fixation hearts were dehydrated in an ascending ethanol series in ddH_2O (v/v) of 50 %, 70 and 100 % (Carl Roth, Karlsruhe, Germany) at RT for at least 2 h while shaking. Subsequently, samples were bleached for 4 h in freshly prepared 5 % (v/v) hydrogen peroxide (Sigma Aldrich, St. Louis, MO, USA) and 5 % (v/v) dimethyl sulfoxide (Carl Roth, Karlsruhe, Germany) in 100 % ethanol while standing at 4 °C. After two washing steps of at least 24 h in 100 % ethanol, samples were transfered into pure (99 %) ethyl cinnamate (ECi, Sigma Aldrich, St. Louis, MO, USA) for at least 4 h prior to imaging. Image stacks were acquired using the the Ultramicroscope Blaze (Miltenyi Biotec, Bergisch Gladbach, Germany) and the analysis was conducted using Imaris 9.3 (Oxford Instruments, Abingdon, United Kingdom).

2.9. Western blot

Hearts were incubated in RIPA buffer comprised of 1 % NP40 (Sigma, St. Louis, MO, USA), 150 mM NaCl (Carl Roth, Karlsruhe, Germany), 0.5 mM EDTA (Carl Roth, Karlsruhe, Germany), 50 mM TRIS-HCL (Carl Roth, Karlsruhe, Germany) and 1 % protease/phosphatase inhibitor (ThermoFisher Scientific, Waltham, MA, USA) in PBS^{-Ca-Mg} (pH = 7.4) for 1 h at 4 °C on a rotor at 20 r.p.m. following mechanical mincing. Afterwards, suspensions were centrifuged centrifuged at 20,000 × *g* for 15 min at 4 °C and supernatants were stored at −80 °C until further analysis. Protein concentration was determined by using a Bradford Assay (Bio-Rad, Hercules, CA, USA). 20 µg protein per sample were transferred to a 4–12 % Bis-Tris-Glycine gel (Invitrogen, Waltham, MA, USA). SDS-PAGE was run at a constant 120 V for 80 min. Separated proteins were dry transferred from the gel to a nitrocellulose membrane using the iBlot2 system (Invitrogen, Waltham, MA, USA) at P0 (20 V for 1 min, 23 V for 4 min, 25 V for 2 min). For whole protein stain, Ponceau S staining (Sigma-Aldrich, St. Louis, MO, USA) was conducted and visualised using the Amersham 680 Imager (GE LifeScience, Washington, DC, USA). Afterwards, membranes were then blocked with 3 % bovine serum albumin (Carl Roth, Karlsruhe, Germany) in tris-buffered saline comprised of 10 mM TRIS (Carl Roth, Karlsruhe, Germany), 100 mM NaCl (Carl Roth, Karlsruhe, Germany) and 2 % Tween-20 (Carl Roth, Karlsruhe, Germany) in ddH_2O at pH 7.5 (TBS-T buffer) for 1 h at RT. Staining was conducted in a new change of the same buffer with 3 % bovine serum albumin over night at 4 °C with monoclonal anti-mouse CD47 (rat, clone: mIAP301, 1:1000, Santa Cruz, Dallas, TX, USA). Membranes were washed three times in TBS-T buffer at RT and then secondary antibodies conjugated with horse radish peroxidase were added in TBS-T buffer plus 3 % bovine serum albumin (Carl Roth, Karlsruhe, Germany) for 1 h at RT (anti-rat, 1:5000, Abcam, Cambridge, UK). Afterwards, membranes were washed three times in TBS-T buffer and imaged using an Amersham 680 Imager (GE LifeSciences, Washington, DC, USA) with SuperSignal™ West Femto Maximum Sensitivity Substrat (ThermoFisher Scientific, Waltham, MA, USA). Images were analyzed using ImageJ 1.53 (NIH, New York City, NY, USA) [27]. Intensity values obtained from antibody stainings were first normalized to values from whole protein stains and then normalized to mean values from the control group.

2.10. Immunohistochemistry

Sections of 4 µm myocardial tissue were created from paraffin-embedded formalin-fixated samples. Sections were deparaffinized and rehydrated, followed by antigen retrieval by incubation at 95 °C in Antigen Retrieval Buffer pH 6.0 (Abcam, Cambridge, UK). Samples were then blocked in TRIS-buffered saline with 0,1 % (v/v) Tween-20 (NaCl, TRIS, and Tween-20 (Roth, Karlsruhe, Germany) with 5 % (v/v) normal goat serum (Invitrogen, Carlsbad, CA, USA) for 1 h. Slices were incubated in blocking buffer with the primary antibodies at 4 °C overnight (CD47 (ab218810), rabbit, 1:2000, Abcam, Cambridge, UK; CD31 (DIA-310), rat, 1:20, Dianova, Hamburg, Germany) followed by staining with secondary antibodies at room temperature for 1 h (anti-rabbit AlexaFluor680, 1:200; anti-rat Cy3, 1:200, both Invitrogen, Carlsbad, CA,

USA). Nuclei were stained with DAPI 1:5000 (1:5000 in TBS-T, Invitrogen, Carlsbad, CA, USA) followed by preservation in Prolong gold antifade reagent (Invitrogen, Carlsbad, CA, USA). Images were acquired using an Olympus BX51 microscope (Olympus, Shinjuku, Japan) and processed using ImageJ software.

2.11. In vitro phagocytosis assay

For neutrophil isolation, bone marrow of baseline C57Bl/6JRJ mice, 12 ± 3 weeks of age without any antibody treatment was flushed and resuspended in 3 mL red blood cell (RBC) lysis buffer (0.15 M NH_4Cl (Carl Roth, Karlsruhe, Germany), 0.1 M $NaHCO_3$ (Carl Roth, Karlsruhe, Germany) and 0.1 mM EDTA dissodium (Merck-Millipore, Burlington, MA, USA) dissolved in ddH_2O, pH = 7.3) and incubated for 5 min while standing at room temperature. Afterwards, cells were centrifuged at 300 × *g* and room temperature for 10 min and resuspended in 200 μL MACS buffer (2 mM EDTA (Invitrogen, Waltham, MA, USA) and 1 % (v/v) fetal bovine serum (PAN-Biotech, Aidenbach, Germany) in PBS) following neutrophil isolation according to the protocol of the murine neutrophil isolation kit by Miltenyi (Bergish Gladbach, Germany). Finally, isolated neutrophils were resuspended in RPMI medium (Gibco, Waltham, MA, USA) containing 100 U/ml penicillin/0.1 mg/ml streptomycin (Sigma Aldrich, St. Louis, MO, USA), 1x NEAA (Sigma Aldrich, St. Louis, MO, USA), 10 mM HEPES (Sigma Aldrich, St. Louis, MO, USA) and 1 mM sodium pyruvat (Sigma Aldrich, St. Louis, MO, USA).

To generate apoptotic cardiomyocytes, C57Bl/6JRJ mice were killed by cervical dislocation in isoflurane narcosis and hearts were perfused *in situ* for 2 min with EDTA buffer (130 mM NaCl (Sigma Aldrich, St. Louis, MO, USA), 5 mM KCl (Carl Roth, Karlsruhe, Germany), 0.5 mM NaH_2PO_4 (Sigma Aldrich, St. Louis, MO, USA), 10 mM HEPES (Sigma Aldrich, St. Louis, MO, USA), 10 mM Glucose (Sigma Aldrich, St. Louis, MO, USA), 10 mM Taurin (Sigma Aldrich, St. Louis, MO, USA) and 5 mM EDTA (ThermoFisher Scientific, Waltham, MA, USA) dissolved in ddH_2O, pH = 7.8) using a roller pump (Ismatec, Grevenbroich, Germany) followed by heart extraction and another 6 min *ex vivo* perfusion with the same buffer and clamped aorta. In a next step, hearts were perfused with perfusion buffer (130 mM NaCl (Sigma Aldrich, St. Louis, MO, USA), 5 mM KCl (Carl Roth, Karlsruhe, Germany), 0.5 mM NaH_2PO_4 (Sigma Aldrich, St. Louis, MO, USA), 10 mM HEPES (Sigma Aldrich, St. Louis, MO, USA), 10 mM Glucose (Sigma Aldrich, St. Louis, MO, USA), 10 mM Taurin (Sigma Aldrich, St. Louis, MO, USA) and 1 mM $MgCl_2$ (Carl Roth, Karlsruhe, Germany) dissolved in ddH_2O, pH = 7.8) for 2 min following perfusion with collagenase solution (0.5 mg/ml collagenase II (Worthington, Lakewood, NJ, USA), 0.5 mg/ml collagenase IV (Worthington, Lakewood, NJ, USA) and 0.05 mg/ml protease XIV (Sigma Aldrich, St. Louis, MO, USA) dissolved in perfusion buffer) up to 20 min until heart tissue is digested. Afterwards, aorta and atria were removed and tissue was seperated manually and stop solution (5 % fetal calf serum (Sigma Aldrich, St. Louis, MO, USA) in perfusion buffer) was added and cell suspension was filtered using a 100 μm cell strainer (Falcon, Corning, NY, USA). Subsequently, cardiomyocytes were isolated by gravity settling and resuspended in 0.1 μM Calcein AM (Invitrogen, Waltham, MA, USA) following incubation at room temperature for 20 min. Next, cells were centrifuged at 300 × *g* and 4 °C for 5 min and resuspended in 2 μM staurosporine solution (Sigma Aldrich, St. Louis, MO, USA) to induce apoptosis. After an incubation for 2 h at 37 °C and 5 % CO_2, apoptotic cardiomyocytes were centrifuged at 800 × *g* and 4 °C für 10 min and resuspended in RPMI medium.

After isolation, neutrophils and apototic cardiomyocytes were co-incubated in a ratio of 1:5 (200.000 neutrophils to 1 × 10^6 apoptotic cardiomyocytes) for 1 h at 37 °C and 5 % CO_2 with either 0.1 μg/μl anti-CD47 antibody (clone: clone: mIAP301) or corresponding IgG2a Isotype control antibody (clone: RTK2758; both BioLegend, San Diego, CA, USA) added. Afterwards, cells were centrifuged at 450 × *g* and 4 °C for 5 min and Fc-receptor blocking and staining with Ly6G-BV421 (1:200; BioLegend, San Diego, CA, USA) was conducted as mentioned above and cells were finally resuspended in 200 μL FACS buffer for flow cytometry analysis.

2.12. Statistics

Statistical analysis was conducted using Graphpad Prism 6 (Graphpad Software, Boston, MA, USA). All graphs show every biological individual analyzed, in addition to the mean and standard deviation of the respective group. After testing for Gaussian distribution tests were chosen accordingly (Student's *t*-test for single comparison and ANOVA with Bonferroni correction for multiple comparisons) as stated in the respective figure legend. Correlation was performed using lineary regression best-fit and calculating Pearson's correlation coefficient *r*. A p-value < 0.05 was considered statistically significant and significance levels were marked with asterisks (*: $p < 0.05$, **: $p < 0.01$ **, ***: $p < 0.001$).

3. Results

3.1. CD47 inhibition reduces infarct size in vivo after acute myocardial reperfusion injury

Following CD47 inhibition by antibody blockade, mice showed a reduced area of infarction, measured by triphenyl tetrazolium chloride (TTC) Evan's blue staining, compared to IgG control treated animals (19.47 ± 9.27 % vs. 34.28 ± 10.87 %, $p = 0.048$, Fig. 1A). To evaluate the impact of infiltrating immune cells, we performed *ex vivo* ischemia/reperfusion experiments using an isolated perfused heart system as previously described [28]. $CD47^{-/-}$ mice were examined and compared to wild-type littermates. No significant reduction of infarct size was observed in $CD47^{-/-}$ mice (26.3 ± 6.81 % vs. 24.46 ± 6.29 % (normalized on AAR), $p = 0.64$, Fig. 1B). Similar results were found in hypoxia/reoxygenation experiments performed in human cardiomyocytes (hCM). After 20 h of hypoxia and 4 h of reoxygenation, cell viability was significantly decreased (100 ± 4.42 % vs. 67.02 ± 4.41 %, $p = 0.0002$, Fig. 1C). However, additional CD47 inhibition did not affect this decrease in cell viability (67.02 ± 4.41 % vs. 65.31 ± 3.14 %, $p = 0.62$, Fig. 1C).

3.2. CD47 inhibition showed higher neutrophils count per infarct size volume

Differences between *in vivo* and *ex vivo* investigations suggested an influence of immune cells during CD47 inhibition. Therefore, we performed flow cytometry analysis. After 24 h of reperfusion, we observed a neutrophil dominant immune cell infiltration, but in mice treated with anti-CD47 antibody, no differences were found in neutrophil (3241 ± 2531 cells/mg tissue vs. 3972 ± 1904 cells/mg heart, p = 0.84, Fig. 2A), macrophage (1018 ± 841 cells/mg heart vs. 1427 ± 720 cells/mg heart, p = 0.98, Fig. 2A), monocyte (1616 ± 788 cells/mg heart vs. 2184 ± 396 cells/mg heart, p = 0.93, Fig. 2A) and lymphocyte count (1185 ± 623 cells/mg heart vs. 814 ± 248 cells/mg heart, p = 0.99, Fig. 2A) compared to control group. To elucidate the spatial organization of the infiltrating neutrophils, we performed light sheet fluorescence microscopy (LSFM). For detection of the infarcted area, we used CD31 staining via intravenous tail vein injection of a fluorophore-conjugated antibody as previously described as $CD31^{neg}$ myocardial reperfusion injury [26]. Three-dimensional imaging revealed a reduction in $CD31^{neg}$ volume (2.63 ± 1.94 % vs. 7.17 ± 3.22 % (normalized to total heart volume), p = 0.03, Fig. 2B and 2C), matching observations made using TTC Evan's blue staining (Fig. 1A). Furthermore, we performed LSFM-based neutrophil staining using a fluorophore-conjugated anti-Ly6G antibody. This revealed an infiltration of neutrophil granulocytes, mostly located around the $CD31^{neg}$ volume (Fig. 2B). Similar to results made by flow cytometry, no significant difference in absolute neutrophil count could be observed (82902 ± 43255 $Ly6G^+$ spots/heart vs. 120700 ±

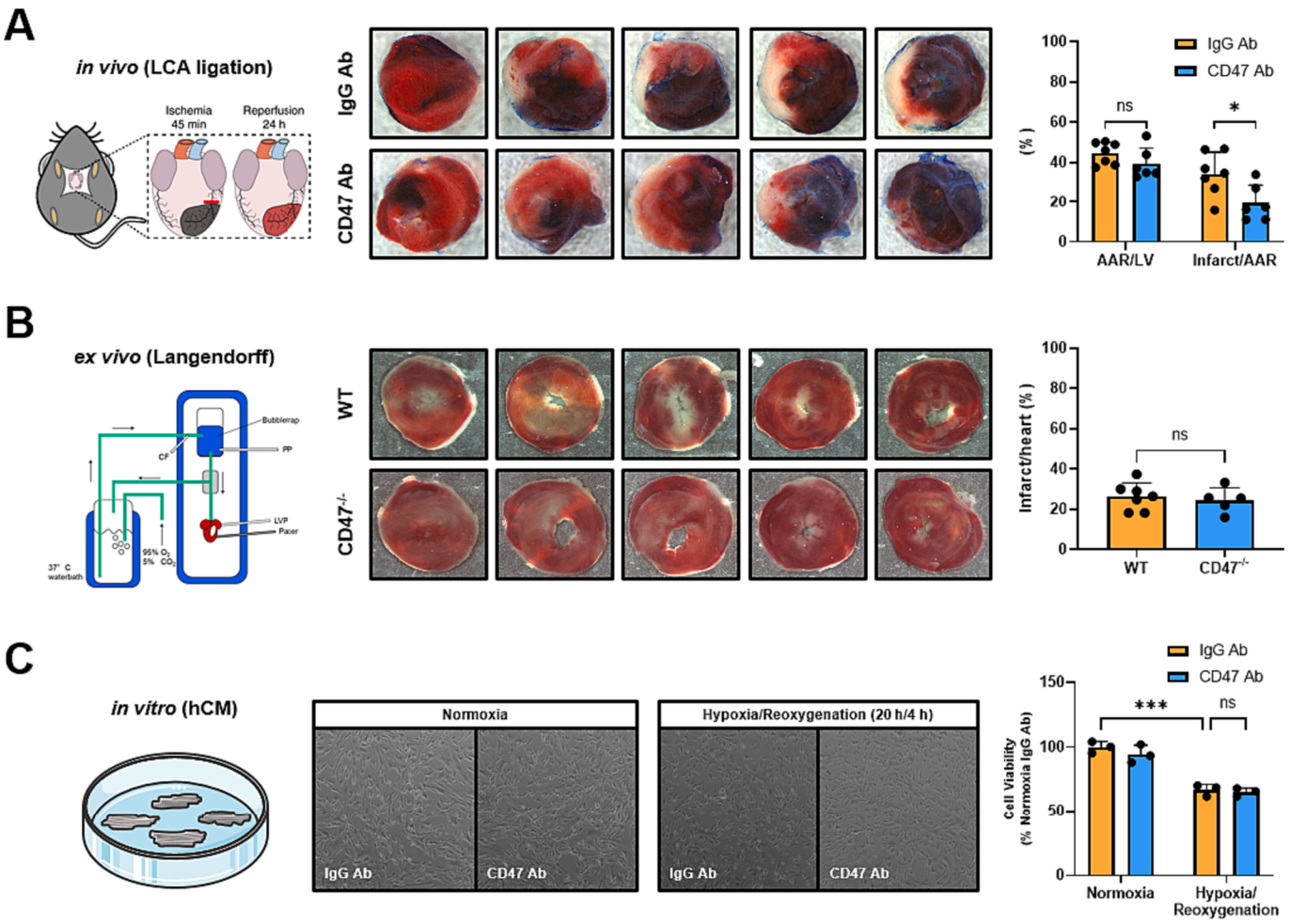

Fig. 1. Effects of CD47 inhibition on infarct size *in vivo* and *ex vivo*. (A) Left: Graphical abstract of *in vivo* ischemia/reperfusion injury procedure. Middle: Exemplary cardiac TTC Evan's blue staining of mice treated with anti-CD47 antibody (CD47 Ab, bottom row) or IgG isotype control (IgG Ab, top row) after 45 min of ischemia and 24 h of reperfusion. Right: Size comparison of area at risk (AAR, normalized to left ventricle (LV)) and infarct area (normalized to AAR) (n = 6–7, Student's *t*-test with Welch correction, *: $p < 0.05$). (B) Left: Schematic illustration of Langendorff setup. Middle: Exemplary heart slices of wild-type (WT, top row) and $CD47^{-/-}$ knockout mice (bottom row) after *ex vivo* ischemia/reperfusion. Right: Comparison of infarct size of WT and$CD47^{-/-}$ mice after *ex vivo* ischemia/reperfusion (n = 5–7, Student's *t*-test with Welch correction). (C) Left/Middle: Exemplary pictures of human cardiomyocytes (hCM) under normoxia or after *in vitro* hypoxia/reoxygenation with either anti-CD47 treatment (CD47 Ab) or IgG isotype control (IgG Ab) respectively. Right: Comparison of cell viability (normalized to viability of cells treated with IgG isotype control under normoxia) between anti-CD47 treated cells and control group under normoxia or after hypoxia/reoxygenation (n = 3, ANOVA with Bonferroni post-hoc test, ***: $p < 0.001$). ns: not significant. (For interpretation of the references to color in this figure legend, the reader is referred to the web version of this article.)

66459 $Ly6G^+$ spots/heart, $p = 0.426$, Fig. 2C). Interestingly, normalization to size of injury volume ($CD31^{neg}$ volume) exposed an increased number of associated neutrophil under CD47 inhibition compared to control group (38306 ± 11655 $Ly6G^+$ spots/mm^3 $CD31^{neg}$ volume vs. 18397 ± 15033 $Ly6G^+$ spots/mm^3 $CD31^{neg}$ volume, $p = 0.049$, Fig. 2C). Additionally, we observed a significant positive correlation between neutrophil count and injury volume in mice treated with anti-CD47 antibody ($r = 0.9658$, $p = 0.0075$, Fig. 2C). The portion of neutrophils associated with the $CD31^{neg}$ injury volume showed no significant difference between mice treated with anti-CD47 antibody and the control group (49.1 % ± 28.0 % vs. 32.5 % ± 17.6 %, Fig. 2D).

3.3. CD47 inhibition increases neutrophil phagocytotic activity of apoptotic cardiomyocytes

To examine underlying mechanisms explaining reduction in infarct size, we first analyzed CD47 expression in hearts at baseline as well as after acute ischemia/reperfusion. In the baseline murine heart we found cardiomyocytes, fibroblasts and endothelial cells to carry CD47, the latter showing most prominent expression (10.39 ± 2.6 fold increase (endothelial cells) and 1.3 ± 0.8 fold increase (cardiomyocytes) to fibroblasts, $p = 0.0001$, Fig. 3A). Compared to baseline, we observed an increase in CD47 expression in whole heart lysates after 45 min of ischemia following 24 h of reperfusion, measured by western blot (181.8 % ± 49.5 % vs. 100 % ± 21.1 %, $p = 0.008$, Fig. 3B). Using immunohistochemistry, we also found CD47 to be mostly increased in the $CD31^{neg}$ infarcted area (Fig. 3C). Furthermore, we examined impact of CD47 inhibition on phagocytotic activity of isolated bone marrow neutrophils in co-incubation with apoptotic, Calcein AM-labeled cardiomyocytes using flow cytometry. Here, we found an enhanced engulfment of cardiomyocytes by neutrophils after CD47 inhibition, reflected by an increased percentage of $Calcein\text{-}AM^+$ neutrophils (3.08 % ± 0.38 % vs. 2.49 % ± 0.36 %, $p = 0.03$, Fig. 3D).

4. Discussion

Our study shows that CD47 blockade reduces infarct size after repAMI *in vivo*. Interestingly, this effect was not observed in *ex vivo* or *in*

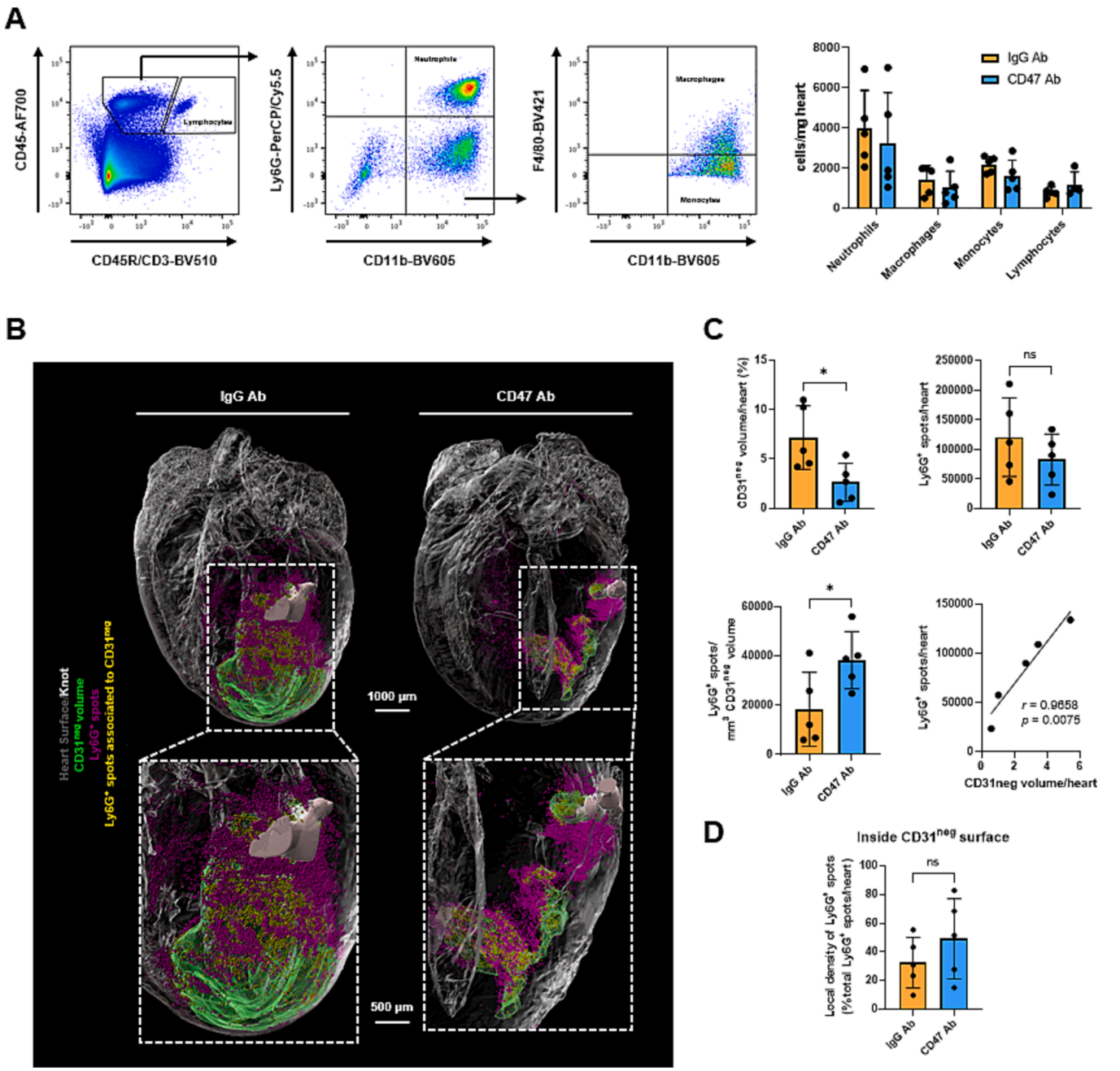

Fig. 2. Effects of CD47 inhibition on cardiac immune cell infiltration after repAMI. (A) Left: Exemplary pseudo-color dot plots for separation of immune cell populations in heart tissue using flow cytometry. Right: Number of neutrophils ($CD45^+$, $Ly6G^+$, and $CD11b^+$), macrophages ($CD45^+$, $Ly6G^-$, $CD11b^+$ and $F4/80^+$), monocytes ($CD45^+$, $Ly6G^-$, $CD11b^+$ and $F4/80^-$) and lymphocytes ($CD45^+$ and $CD45R/CD3^+$) in heart tissue of mice treated either with anti-CD47 or IgG isotype control antibody (n = 5, Student's *t*-test with Welch correction). (B) Exemplary three-dimensional (3D) visualization of $CD31^{neg}$ volume and $Ly6G^+$ spots. (C) Analysis of LSFM-based measurements of myocardial injury volume ($CD31^{neg}$ volume) and neutrophil count ($Ly6G^+$ spots) in mice after CD47 inhibition and control animals. Top left: Quantitative size comparison of $CD31^{neg}$ volume per heart (n = 5, Student's *t*-test with Welch correction, *: $p < 0.05$). Top right: Number of $Ly6G^+$ spots per heart (n = 5, Student's *t*-test with Welch correction). Bottom left: Normalization of $Ly6G^+$ spots count to $CD31^{neg}$ volume (n = 5, Student's *t*-test with Welch correction, *: $p < 0.05$). Bottom right: Correlation of $Ly6G^+$ spots with $CD31^{neg}$ volume per heart (n = 5, *r*- and *p*-values depicted). (D) Local density of $Ly6G^+$ spots associated to myocardial injury volume within 50 µm of $CD31^{neg}$ border (n = 5, Student's *t*-test with Welch correction). ns = not significant.

vitro models, suggesting an extracardial impact evoking the reduction in tissue damage. In addition, CD47 inhibition does not alter absolute number of infiltrating immune cells after 24 h of reperfusion, but, compared to injury size, relatively more neutrophils were associated with the injured area. Furthermore, CD47 was increased in cardiac tissue homogenates after repAMI and blockade of CD47 enhances neutrophil phagocytotic activity of cardiomyocytes debris *in vitro*, which could be an underling mechanism for acute reduction of infarct size after repAMI *in vivo*.

CD47 inhibition is known to reduce injury size *in vivo* in different ischemia/reperfusion models. In organ transplant models, CD47 blockade reduced ischemia/reperfusion injury by decreasing ROS production, inflammatory cytokines and immune cell infiltration [21,22,29]. During renal ischemia/reperfusion, inhibition of CD47 decreased tissue damage through upregulation of self-renewal transcription factors [30]. In a model of transient focal cerebral ischemia,

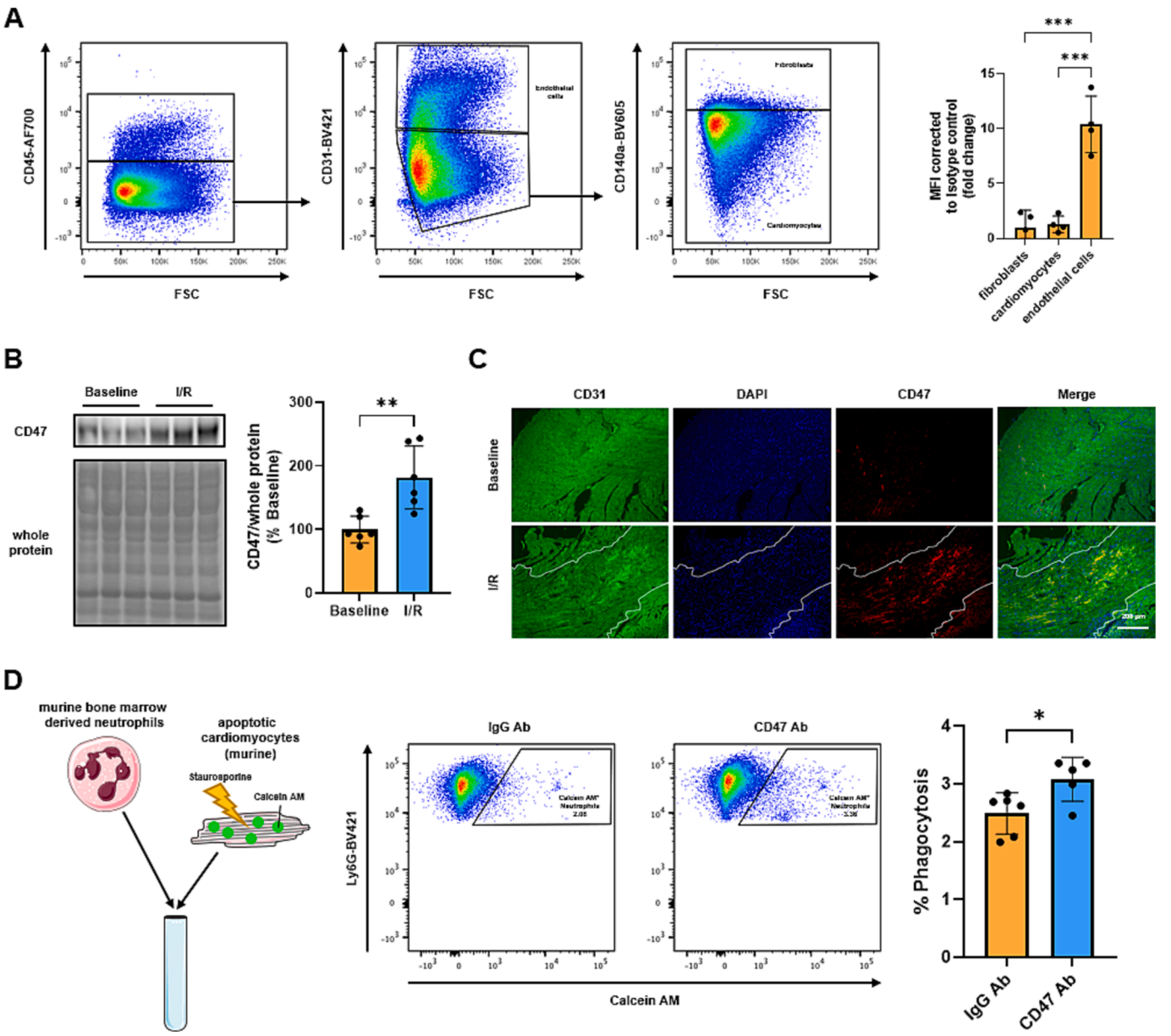

Fig. 3. Baseline expression of CD47 on cardiac cells and effects of anti-CD47 treatment on phagocytotic activity of neutrophils. (A) Measurement of CD47 expression in baseline murine hearts. Left: Exemplary pseudo-color dot plots for separation of cell populations in heart tissue using flow cytometry. Right: Mean fluorescence intensity (MFI) corrected to isotype control of endothelial cells ($CD45^-$ and $CD31^+$), fibroblasts ($CD45^-$, $CD31^-$ and $CD140a^+$) and cardiomyocytes ($CD45^-$, $CD31^-$ and $CD140a^-$) in murine baseline heart tissue depicted as fold change relative to fibroblasts (n = 4, ANOVA with Bonferroni post-hoc test, ***: $p < 0.001$). (B) Left: Western blot micrographs of CD47 of whole cardiac tissue lysates from baseline and ischemia/reperfusion (I/R) hearts with corresponding whole protein stain. Right: Quantified expression of CD47 from micrographs on the left normalized to baseline group (n = 6, Student's *t*-test with Welch correction, **: $p < 0.01$). (C) Representative data from immunofluorescence imaging in mouse hearts 24 h following I/R. The endothelial cell marker CD31 is shown in green, nuclei (DAPI) in blue and CD47 in red. The infarct zone is identified by a decrease in CD31 expression (white edging). (D) Left: Graphical abstract of *in vitro* neutrophil phagocytosis assay. Middle: Exemplary pseudo-color dot plots of Calcein AM^+ neutrophils after co-incubation with Calcein AM-labeled apoptotic cardiomyocytes using flow cytometry. Right: Quantification of percent phagocytosis of Calcein-AM labeled apoptotic cardiomyocytes by neutrophils (n = 5–6, Student's *t*-test with Welch correction, *: $p < 0.05$). (For interpretation of the references to color in this figure legend, the reader is referred to the web version of this article.)

reduction of injury size provoked by CD47 knockout was associated with decreased neutrophil infiltration and MMP-9 level [31]. There is also evidence, that inhibition of CD47 signaling reduces infarct size during repAMI in mice and rats [20,32]. Here, the authors attribute this protective effect to either enhanced phagocytosis by macrophages [20] or reduced oxidative stress [32]. Of note, our study underlines the importance of immune cell infiltration facilitating protective effects of CD47 blockade during repAMI, shown by discrepancy between *in vivo* and *ex vivo/in vitro* results. However, in most ischemia/reperfusion models, anti-CD47 therapy reduced absolute immune cell infiltration, which we did not observe after repAMI. Nevertheless, these changes in immune cell infiltration are only reported for later time points than 24 h of reperfusion [21,22,31,33]. After repAMI, others also could not observe any changes in immune cell infiltration after 24 h of reperfusion [20].

CD47 is a ubiquitous expressed cell surface protein serving as a protection against the innate immune system ("don't eat me" signal). Formerly discovered in immune cell evasion mechanisms of different cancer entities [34–37], it was similarly found to be upregulated during ischemia/reperfusion, as we also observed in our study [20,22,32]. Although inhibition has protective effects, there is also some evidence,

that CD47 expression is essential for tissue repair after damage [38].

Another important function of CD47 is controlling phagocytotic activity of immune cells [11]. As others reported before, CD47 inhibition enhances phagocytosis in macrophages [13,14,20] while CD47 overexpression leads to a decrease [39]. Our experiments revealed that cardiomyocytes, fibroblasts and endothelial cells express CD47 in the baseline murine heart, the latter with the most prominent expression levels. Given the fact that endothelial cells are in direct contact with circulating immune cells, this high level of CD47 expression is rather presumable. Nevertheless, it has been forwarded that during reperfused acute myocardial infarction (repAMI) the majority of damaged cardiac cells and cellular debris is derived from cardiomyocytes, as these cells make up the majority of the heart tissue biomass and are more vulnerable to ischemia/reperfusion injury compared to other cell types [40]. Based on that, we first show anti-CD47 therapy to be capable of increasing phagocytosis of cardiac cell debris by neutrophils. It is also tempting to speculate that this CD47-dependent phagocytosis takes mainly place in the infarcted region as our LSFM-based analysis showed the main portion of infiltrating neutrophils associated to the injury volume. Furthermore, we and others found CD47 to be mostly increased in the infarct region [20].

During repAMI, it has been described that CD47 blockade enhances phagocytotic activity by macrophages [20]. Our study provides additional knowledge showing anti-CD47 treatment to increase phagocytosis of cardiac cell debris by neutrophils, too. Differences between *in vivo* and *ex vivo* investigations do not support a possible enhanced phagocytosis activity by resident cardiac immune cells after repAMI. Comparing the rates of phagocytosis, we found a phagocytosis rate of 2 % for neutrophils, while others described rates of 20 % for macrophages [20]. However, anti-CD47 treatment reduces infarct size already after 24 h of reperfusion. As neutrophils show their peak of infiltration after 24 h of reperfusion, in contrast to macrophages mainly infiltrating into the heart after 3 to 5 days of reperfusion, enhanced phagocytosis by neutrophils under anti-CD47 treatment might play a relevant role in reducing infarct size [41,42].

Our study only provides *in vitro* data on neutrophil phagocytosis. Therefore, direct *in vivo* investigations of phagocytotic activity of infiltrated cardiac neutrophils are needed as further evidence. As another limitation there is also to mention, that functional analysis and long-term experiments are missing to examine the impact of CD47 blockade on cardiac function and remodeling after repAMI. Furthermore, additional analysis of immune cell function and infiltration at later time points are needed to understand the effects on subsequent inflammatory and reparative processes.

Our study is the first to show enhanced phagocytosis of cardiac cell debris by neutrophils through CD47 inhibition. We suggest that this could contribute to an injury reduction after repAMI, highlighting anti-CD47 treatment as an interesting target for protective therapy in this context. Further investigations are needed to elucidate the impact of altered phagocytosis by neutrophils during repAMI. Besides, translational research is necessary to provide the basis for improved patient care in future projects.

Funding

This work was supported by German Cardiac Society (DGK, Deutsche Gesellschaft für Kardiologie – Herz- und Kreislaufforschung e.V.) under Grant DGK02/2022 and Universitätsmedizin Essen Clinical Scientist Acedemy (UMEA) Junior Fellowship to E.H.-Y. The German Research Foundation also supported this work under Grant HE6317/2-1 to U.B. H.-C. and Grant RA969/12-1 to T.R.

CRediT authorship contribution statement

Elias Haj-Yehia: Conceptualization, Methodology, Software, Validation, Formal analysis, Investigation, Resources, Data curation, Writing – original draft, Visualization, Funding acquisition. **Sebastian Korste:** Conceptualization, Methodology, Software, Validation, Formal analysis, Investigation, Resources, Data curation, Writing – original draft, Visualization, Supervision, Project administration. **Robert Jochem:** Investigation. **Aldona Lusha:** Software, Validation, Formal analysis, Investigation. **Anna Roth:** Methodology, Investigation. **Nina Dietzel:** Investigation. **Josefine Niroomand:** Investigation. **Pia Stock:** Software, Validation. **Astrid M. Westendorf:** Investigation, Supervision. **Jan Buer:** Supervision. **Ulrike B. Hendgen-Cotta:** Resources, Writing – review & editing, Supervision, Project administration, Funding acquisition. **Tienush Rassaf:** Resources, Writing – review & editing, Supervision, Project administration, Funding acquisition. **Matthias Totzeck:** Conceptualization, Resources, Writing – review & editing, Supervision, Project administration.

Declaration of Competing Interest

The authors declare the following financial interests/personal relationships which may be considered as potential competing interests: M.T. and T.R. report personal fees and others from Edwards and Novartis, Bristol Myers Squibb, Bayer, Daiichi Sankyo and Astra Zeneca, which are outside the submitted work. All other authors declare no conflict of interest. T.R. and U.B.H.-C. cofounded Bimyo, a company focusing on cardioprotection.

Acknowledgments

We thank the staff of the Imaging Center Essen (IMCES) for their continuous technical support and the usage of their instruments. We also acknowledge the use of elements from Servier Medical Art, provided by Servier, licensed under a Creative Commons Attribution 3.0 unported license.

Appendix A. Supplementary material

Supplementary data to this article can be found online at https://doi.org/10.1016/j.ijcha.2023.101269.

References

[1] N.G. Frangogiannis, Inflammation in cardiac injury, repair and regeneration, Curr. Opin. Cardiol. 30 (3) (2015) 240–245.
[2] S.L. Puhl, S. Steffens, Neutrophils in post-myocardial infarction inflammation: damage vs resolution? Front. Cardiovasc. Med. 6 (2019) 25.
[3] Y. Ma, Role of neutrophils in cardiac injury and repair following myocardial infarction, Cells 10 (7) (2021).
[4] M. Horckmans, et al., Neutrophils orchestrate post-myocardial infarction healing by polarizing macrophages towards a reparative phenotype, Eur. Heart J. 38 (3) (2017) 187–197.
[5] F. Carbone, A. Bonaventura, F. Montecucco, Neutrophil-related oxidants drive heart and brain remodeling after ischemia/reperfusion injury, Front. Physiol. 10 (2019) 1587.
[6] Y. Doring, O. Soehnlein, C. Weber, Neutrophil extracellular traps in atherosclerosis and atherothrombosis, Circ. Res. 120 (4) (2017) 736–743.
[7] Y. Doring, P. Libby, O. Soehnlein, Neutrophil extracellular traps participate in cardiovascular diseases: recent experimental and clinical insights, Circ. Res. 126 (9) (2020) 1228–1241.
[8] N.G. Frangogiannis, The immune system and the remodeling infarcted heart: cell biological insights and therapeutic opportunities, J. Cardiovasc. Pharmacol. 63 (3) (2014) 185–195.
[9] E. Wan, et al., Enhanced efferocytosis of apoptotic cardiomyocytes through myeloid-epithelial-reproductive tyrosine kinase links acute inflammation resolution to cardiac repair after infarction, Circ. Res. 113 (8) (2013) 1004–1012.
[10] P. Panizzi, et al., Impaired infarct healing in atherosclerotic mice with Ly-6C(hi) monocytosis, J. Am. Coll. Cardiol. 55 (15) (2010) 1629–1638.
[11] R. Maute, J. Xu, I.L. Weissman, CD47-SIRPalpha-targeted therapeutics: status and prospects, Immunooncol. Technol. 13 (2022), 100070.
[12] M. Zhang, et al., Anti-CD47 treatment stimulates phagocytosis of glioblastoma by M1 and M2 polarized macrophages and promotes M1 polarized macrophages in vivo, PLoS One 11 (4) (2016), e0153550.
[13] Y. Kojima, et al., CD47-blocking antibodies restore phagocytosis and prevent atherosclerosis, Nature 536 (7614) (2016) 86–90.
[14] K.U. Jarr, et al., Effect of CD47 Blockade on Vascular Inflammation, N. Engl. J. Med. 384 (4) (2021) 382–383.

[15] D. Candas-Green, et al., Dual blockade of CD47 and HER2 eliminates radioresistant breast cancer cells, Nat. Commun. 11 (1) (2020) 4591.
[16] M.P. Chao, et al., Therapeutic targeting of the macrophage immune checkpoint CD47 in myeloid malignancies, Front. Oncol. 9 (2019) 1380.
[17] N. Dizman, E.I. Buchbinder, Cancer therapy targeting CD47/SIRPalpha, Cancers (Basel) 13 (24) (2021).
[18] D. Tseng, et al., Anti-CD47 antibody-mediated phagocytosis of cancer by macrophages primes an effective antitumor T-cell response, PNAS 110 (27) (2013) 11103–11108.
[19] L. Pan, et al., Lack of SIRP-alpha reduces lung cancer growth in mice by promoting anti-tumour ability of macrophages and neutrophils, Cell Prolif. 56 (2) (2023), e13361.
[20] S. Zhang, et al., Acute CD47 blockade during ischemic myocardial reperfusion enhances phagocytosis-associated cardiac repair, JACC Basic Transl. Sci. 2 (4) (2017) 386–397.
[21] X. Wang, et al., CD47 blockade reduces ischemia/reperfusion injury in donation after cardiac death rat kidney transplantation, Am. J. Transplant. 18 (4) (2018) 843–854.
[22] Z.Y. Xiao, et al., CD47 blockade reduces ischemia/reperfusion injury and improves survival in a rat liver transplantation model, Liver Transpl. 21 (4) (2015) 468–477.
[23] M. Totzeck, et al., A practical approach to remote ischemic preconditioning and ischemic preconditioning against myocardial ischemia/reperfusion injury, J. Biol. Methods 3 (4) (2016).
[24] L. Michel, et al., PD1 deficiency modifies cardiac immunity during baseline conditions and in reperfused acute myocardial infarction, Int. J. Mol. Sci. 23 (14) (2022).
[25] P. Luedike, et al., Cardioprotection through S-nitros(yl)ation of macrophage migration inhibitory factor, Circulation 125 (15) (2012) 1880–1889.
[26] S.F. Merz, et al., Contemporaneous 3D characterization of acute and chronic myocardial I/R injury and response, Nat. Commun. 10 (1) (2019) 2312.
[27] C.A. Schneider, W.S. Rasband, K.W. Eliceiri, NIH Image to ImageJ: 25 years of image analysis, Nat. Methods 9 (7) (2012) 671–675.
[28] T. Rassaf, et al., Circulating nitrite contributes to cardioprotection by remote ischemic preconditioning, Circ. Res. 114 (10) (2014) 1601–1610.
[29] M. Xu, et al., Anti-CD47 monoclonal antibody therapy reduces ischemia-reperfusion injury of renal allografts in a porcine model of donation after cardiac death, Am. J. Transplant. 18 (4) (2018) 855–867.
[30] N.M. Rogers, et al., CD47 regulates renal tubular epithelial cell self-renewal and proliferation following renal ischemia reperfusion, Kidney Int. 90 (2) (2016) 334–347.
[31] G. Jin, et al., CD47 gene knockout protects against transient focal cerebral ischemia in mice, Exp. Neurol. 217 (1) (2009) 165–170.
[32] H.B. Wang, et al., RNAi-mediated down-regulation of CD47 protects against ischemia/reperfusion-induced myocardial damage via activation of eNOS in a rat model, Cell. Physiol. Biochem. 40 (5) (2016) 1163–1174.
[33] J.B. Maxhimer, et al., Thrombospondin-1/CD47 blockade following ischemia-reperfusion injury is tissue protective, Plast. Reconstr. Surg. 124 (6) (2009) 1880–1889.
[34] J. Huang, et al., Role of CD47 in tumor immunity: a potential target for combination therapy, Sci. Rep. 12 (1) (2022) 9803.
[35] M.P. Chao, et al., Anti-CD47 antibody synergizes with rituximab to promote phagocytosis and eradicate non-Hodgkin lymphoma, Cell 142 (5) (2010) 699–713.
[36] S.B. Willingham, et al., The CD47-signal regulatory protein alpha (SIRPa) interaction is a therapeutic target for human solid tumors, PNAS 109 (17) (2012) 6662–6667.
[37] K. Weiskopf, et al., CD47-blocking immunotherapies stimulate macrophage-mediated destruction of small-cell lung cancer, J. Clin. Invest. 126 (7) (2016) 2610–2620.
[38] M. Reed, et al., Epithelial CD47 is critical for mucosal repair in the murine intestine in vivo, Nat. Commun. 10 (1) (2019) 5004.
[39] L. Barrera, et al., CD47 overexpression is associated with decreased neutrophil apoptosis/phagocytosis and poor prognosis in non-small-cell lung cancer patients, Br. J. Cancer 117 (3) (2017) 385–397.
[40] A.K. Singhal, et al., Role of endothelial cells in myocardial ischemia-reperfusion injury, Vasc. Dis. Prev. 7 (2010) 1–14.
[41] Z. Zhang, et al., Mesenchymal stem cells promote the resolution of cardiac inflammation after ischemia reperfusion via enhancing efferocytosis of neutrophils, J. Am. Heart Assoc. 9 (5) (2020), e014397.
[42] V. Rusinkevich, et al., Temporal dynamics of immune response following prolonged myocardial ischemia/reperfusion with and without cyclosporine A, Acta Pharmacol. Sin. 40 (9) (2019) 1168–1183.

DOI: 10.1016/j.ijcha.2023.101269
URN: urn:nbn:de:hbz:465-20231011-092842-0